Tobias Knopp*, Fabian Mohn, Fynn Foerger, Florian Thieben, Niklas Hackelberg, Jonas Faltinath, Artyom Tsanda, Marija Boberg, and Martin Möddel

Empirical Study of Magnet Distance on Magneto-Mechanical Resonance Frequency

https://doi.org/10.1515/cdbme-2024-2092

Abstract: Determining the position and orientation of a medical instrument is essential for accurate procedures in endoscopy, surgery, and vascular interventions. Recently, a novel sensor based on torsional pendulum-like magneto-mechanical motion has been proposed. This sensor is passive, wireless and inductively coupled to a transmit-receive coil array. This setup allows the determination of all 6 degrees of freedom using the characteristic resonance of the sensor. Additional physical quantities such as temperature and pressure can be measured based on the frequency of the sensor, which mainly depends on the distance between the two involved permanent magnets. In this study, we analyze a sensor composed of two magnetic cylinders with variable magnet-to-magnet distance and a basic physical model based on a dipole assumption. Experimental analysis of the resonance frequency and comparison with the model values show both qualitative and quantitative agreement with an average relative error of only 0.8 %. This validates the implemented model and shows the suitability of our magnetic-mechanical resonator made from cylindrical permanent magnets for sensing applications.

Keywords: Magneto-Mechanical Resonator, Sensing, Resonance Frequency, Magnet-to-Magnet Distance

1 Introduction

In modern medical procedures such as endoscopy, surgery, and vascular interventions, accurate determination of the position and orientation of medical instruments is critical [1, 2]. Recently, a novel sensor based on magneto-mechanical resonance has been introduced [3]. This passive and wireless sensor allows 6 degrees of freedom tracking and the sensing of additional physical parameters such as temperature and pressure. A similar approach for combined tracking and actuation was recently proposed [4].

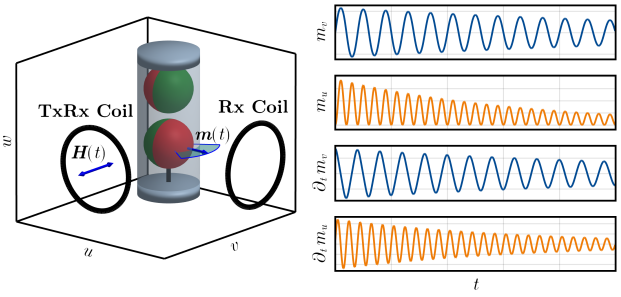

Fig. 1: The basic principle of the magneto-mechanical resonator is illustrated for two magnetic spheres. The upper permanent magnet is fixed, while the lower one is attached to a thin filament shown in black. An electromagnetic coil oriented in v-direction is used to excite the suspended magnet, which then oscillates due to the magnetic torque. The oscillating magnetic moment $\boldsymbol{m}(t)$ of the lower magnet has a component in both the u- and v-directions. Using the induction principle, its time derivative $\partial_t \boldsymbol{m}(t)$ can be detected using the excitation coil in receive mode and an additional receive coil oriented in u-direction.

The tracking and sensing setup proposed in [3] consists of a miniature magneto-mechanical resonator (MMR) and a coil array used to excite and sense the magnetic oscillations. The MMR consists of two attracting permanent magnets in anti-parallel alignment as shown in Fig. 1, one magnet is fixed and the other is attached to a small filament. This configuration allows the suspended magnet to rotate similar to a torsional pendulum with the characteristic resonance frequency f_{MMR}.

The magnetic torque causes the north poles to return to an anti-parallel configuration, while the filament prevents the magnets from being pulled together by their attractive force. We consider a coordinate system where w points in the direction of the filament, u points in the direction of the suspended magnet in equilibrium, and v is orthogonal to w and u. When an external magnetic field $\boldsymbol{H}(t)$ with frequency f_{MMR} is applied in v-direction, it enforces a torque on the suspended magnet, causing it to oscillate. When the external field is switched off, the MMR continues oscillating in a damped angular motion $\boldsymbol{m}(t)$, which is the foundation of remote inductive sensing.

***Corresponding author: Tobias Knopp,** Section for Biomedical Imaging, University Medical Center Hamburg-Eppendorf, Hamburg, Germany, and Institute for Biomedical Imaging, Hamburg University of Technology, Hamburg, Germany, and Fraunhofer Research Institution for Individualized and Cell-Based Medical Engineering IMTE, Lübeck, Germany, e-mail: t.knopp@uke.de

Fabian Mohn, Fynn Foerger, Florian Thieben, Niklas Hackelberg, Jonas Faltinath, Artyom Tsanda, Marija Boberg, Martin Möddel, Section for Biomedical Imaging, University Medical Center Hamburg-Eppendorf, Hamburg, Germany, and Institute for Biomedical Imaging, Hamburg University of Technology, Hamburg, Germany

When using two receive coils in v- and u-directions, the signals in both coils are proportional to the time derivatives $\partial_t m_v(t)$ and $\partial_t m_u(t)$, respectively. In contrast to the v-signal, an orthogonal projection of the pendulum-like motion leads to a u-signal component $m_u(t)$ at twice the frequency. Using a receive coil array as proposed in [3], the full position and orientation information can be reconstructed from the amplitudes of the received signals.

The sensing capabilities of MMRs depend on the coupling of a measurand to the resonance frequency of the sensor. For example, we can measure temperature or pressure by using a housing that changes the magnet-to-magnet distance for that measurand. For two spheres, the change in resonance frequency for varying magnet-to-magnet distance is well understood [3], but this relationship has not been investigated for other magnet geometries. The aim of the present work is to investigate the resonance frequency for cylindrical magnets experimentally and to compare it with predictions derived from a physical model. Possible advantages of cylindrical magnets are their higher fill factor and stronger dipole moment for a cylindrical MMR housing, which in turn increases the signal strength.

2 Methods

We developed an MMR sensor using two cylindrical neodymium magnets (N45) with a diameter of 4 mm and a height of 5 mm and a remanence magnetization of $1.05 \cdot 10^6$ A/m. The cylinders are hollow with a bore diameter of 1.0 mm through which the filament is inserted and glued. One of the magnets is glued to the bottom of the cylindrical housing (acrylic polymer), while the suspended magnet is attached to a ultra-high-molecular-weight polyethylene (PE-UHMW) thread that is connected to a polyethylene screw inserted into the top of the housing that can be adjusted in depth.

For MMR excitation and readout, we have developed a two-channel system consisting of two planar transmit-receive (TxRx) coils, one sensitive for signals in v-direction and the other sensitive in u-direction, as shown in Fig. 2. Both coils are connected to a TxRx circuit, which is responsible for switching between the power amplifier (Xli 2500, Crown) and the data acquisition system with a sampling rate of 61 kHz. This system is based on the STEMlab125-14 (RedPitaya) boards, which have two ADC and two DAC channels, as well as four analog output pins. The latter are used to switch the mode of the setup between transmit and receive. The software of the MMR system uses the RedPitayaDAQServer project [5].

The MMR is placed centrally in front of both coils so that its v-direction aligns with the field generated by the v-coil.

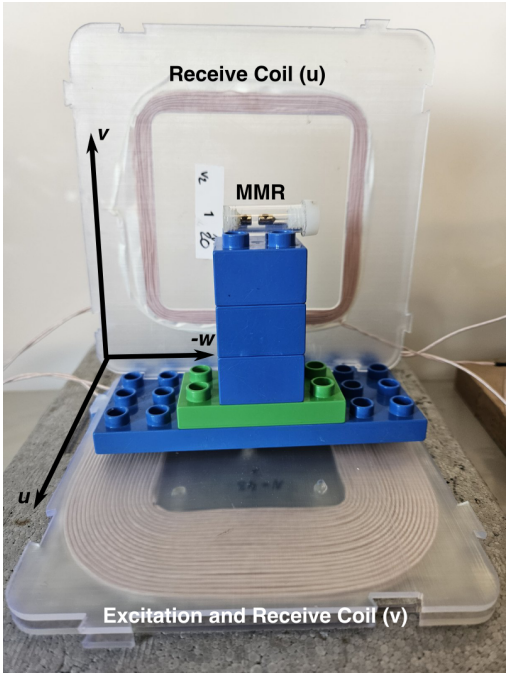

Fig. 2: Experimental setup for excitation and readout of MMR sensor. A planar coil in the uw-plane is used to excite the magneto-mechanical resonator (MMR) with a magnetic field of magnitude $H_v = 0.13\,\mathrm{mT}/\mu_0$ in v-direction. The same coil is then used to read the v-component of the MMR oscillation. In addition, a perpendicular coil in the vw-plane, shown in the background, is responsible for detecting the u-component of the MMR oscillation. The MMR is positioned using interlocking bricks.

Therefore, we only use the v-coil for excitation and set the transmit amplitude of the u-coil to zero. The amplitude of the applied field in the v-coil is $0.13\,\mathrm{mT}/\mu_0$ during excitation for all experiments. This sequence is applied for 30 repetitions and consists of 10 transmit periods and 100 receive periods, with a period length $T_{\mathrm{MMR}} = f_{\mathrm{MMR}}^{-1}$.

The edge-to-edge distance d between the magnets is manually adjusted to eight monotonically increasing values $d \in \{2.7, 3.1, 3.6, 4.3, 4.7, 5.2, 5.7, 6.0\}$ in mm. The distance is measured with a digital caliper. The measurement protocol consisted of four steps: First, the MMR is placed on the sample holder and a rough estimate of the resonance frequency based on the model is used for excitation. Second, the received signal in v-direction is analyzed and the exact resonance frequency is determined. In the third step, the obtained resonance frequency is applied and the MMR is positioned and manually aligned by rotation until the only observed frequency in the orthogonal receive channel u is $2f_{\mathrm{MMR}}$. In the last step, the signal for both channels is simultaneously acquired.

We compare our measurements with the predictions derived from the dipole model presented in the supplementary material of [3]. In short, both cylindrical magnets are mod-

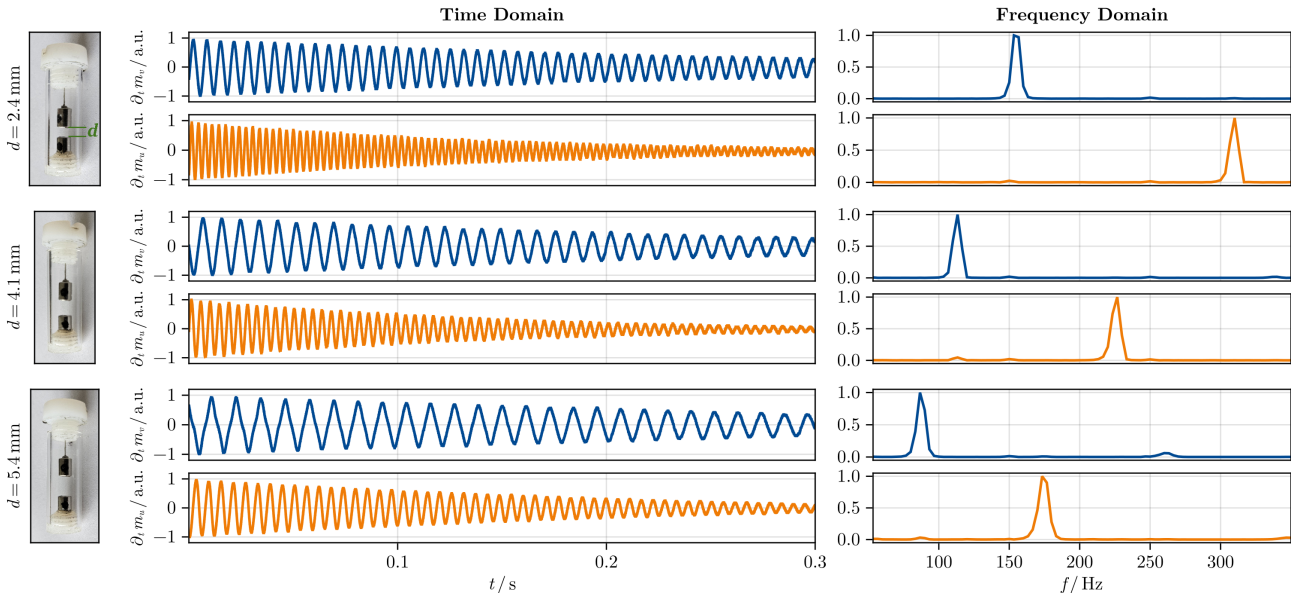

Fig. 3: The receiving coils are arranged in relation to the MMR in such a way that the signals measured at the u- and v-coils are proportional to the components of the time derivative of the magnetic moment of the suspended magnets $\partial_t m_v$ and $\partial_t m_u$ respectively. The first 300 ms of the normalized components $\partial_t m_v$ (blue) and $\partial_t m_u$ (orange) are shown for three selected magnet distances $d \in \{2.7, 4.3, 5.7\}$ in mm in the center column. The first column shows photographs of the MMR. The last column shows the signal in the frequency domain after Hann windowing in the time domain.

eled as point dipoles, with a magnetic dipole moment m at the center of mass of each magnet. The restoring torque on the suspended dipole depends on the magnetic flux density B_0 created by the fixed dipole and the angle φ between the suspended dipole and it's equilibrium state. The dynamic of the magnetic moment is given by

$$\boldsymbol{m}(t) = \begin{pmatrix} m_u(t) \\ m_v(t) \\ m_w(t) \end{pmatrix} = m \begin{pmatrix} \cos\varphi(t) \\ \sin\varphi(t) \\ 0 \end{pmatrix} . \tag{1}$$

The corresponding equation of motion for φ in free oscillation forms a direct realization of a gravitational pendulum

$$mB_0 \sin\varphi + \Gamma\partial_t\varphi + I\partial_t^2\varphi = 0\,, \tag{2}$$

where Γ is the friction constant and I the moment of inertia of a single magnet. In the small angle approximation, it becomes the equation of motion of a harmonic oscillator

$$mB_0\varphi + \Gamma\partial_t\varphi + I\partial_t^2\varphi = 0\,. \tag{3}$$

The resonance frequency of the MMR oscillator is given by

$$\omega_0 = \sqrt{\frac{mB_0}{I}} = \sqrt{\frac{m^2\mu_0}{4\pi d_0^3 I}}\,, \tag{4}$$

where $m = 0.058\,\mathrm{A\,m^2}$, $I = 8.916 \cdot 10^{-10}\,\mathrm{kg\,m^2}$ is the inertia of a hollow cylinder, $B_0 = \frac{m\mu_0}{4\pi d_0^3}$ with $d_0 = d + h$ and $h = 5\,\mathrm{mm}$ is the height of the cylinder magnets. Equation (4) describes the dependency of $\omega_0 \propto d_0^{-\frac{3}{2}}$, to which we compare our measurement results.

3 Results

Fig. 3 shows measured signals for three selected distances $d \in \{2.7, 4.3, 5.7\}$ in mm in time and frequency domain. All signals are normalized for better comparison. In all cases, the signal curve shows a damped oscillation at the MMRs resonance frequency in v-direction and twice the frequency in u-direction. While the waveform is in good sinusoidal approximation for small magnet-to-magnet distances, deviations are noticeable at the larger distances. With increasing d, the magnitude of the third harmonic in the frequency spectrum of the v-channel of the signal increases. This observation indicates a non-linear component within the oscillation that exceeds the limitations of the small angle approximation in (3). This is most likely caused by a decrease in the restoring force of the oscillator at larger magnet distances, which causes the excitation larger amplitudes. We observe that the resonance frequency decreases with increasing distance between the two magnets.

For a quantitative analysis of the resonance frequency shift in dependence of d, the readout of the position of the maximum in the frequency domain signal of the v-channel is taken. Both, the measured and the modeled resonance frequencies are plotted as a function of the magnet-to-magnet distance d and compared in Fig. 4. The frequency at the higher distances is slightly lower than the modeled one. The decrease

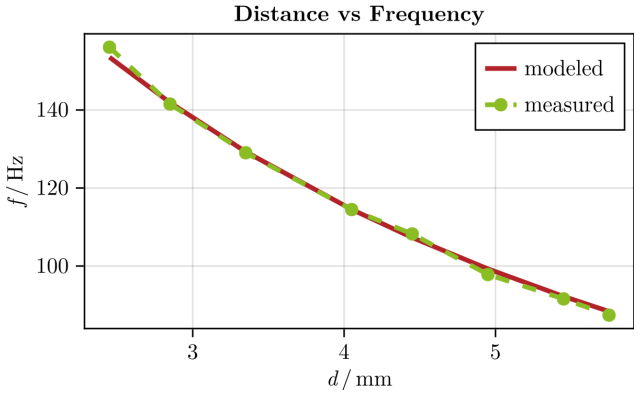

Fig. 4: The plot shows the resonance frequency of both the measured and modeled MMR as a function of the magnet-to-magnet distance.

in the dominance of the attractive force between the magnets at higher distances can explain this effect, causing the suspended magnet to be displaced from the w-axis by gravity. At small distances, the measured resonance frequency is slightly higher than the modeled frequency. This discrepancy could be attributed to the limitations of the dipole approximation for cylinders at small distances. Such observations are not made in the case of spheres, which are identical to the dipole field for all distances outside the sphere [6]. A good agreement with an average relative error over all distances of only 0.8 % can be seen between the modeled and measured frequencies.

4 Conclusion

In this paper we have studied the dependency of the resonance frequency of cylindrical magneto-mechanical resonators on their magnet-to-magnet distance. Despite manual fabrication of the MMR with a higher potential for imperfection in magnet placement and filament attachment, we achieve a strong qualitative and quantitative agreement to a physical dipole model with a mean relative error of 0.8 %. Cylindrical magnets have the potential to improve sensing applications due to their higher frequency gradient with distance, compared to the dipole model of spherical magnets. Our results also highlight the suitability of model-based approaches for sensing applications using magneto-mechanical resonators.

Author Statement

Research funding: This project was partly funded by the Deutsche Forschungsgemeinschaft (DFG) - SFB 1615 - 503850735 - TP B03
Conflict of interest: Authors state no conflict of interest.

References

[1] J. Kaesmacher, J. Gralla, P. J. Mosimann, F. Zibold, M. R. Heldner, E. Piechowiak, T. Dobrocky, M. Arnold, U. Fischer, P. Mordasini. Reasons for reperfusion failures in stent-retriever-based thrombectomy: registry analysis and proposal of a classification system. American Journal of Neuroradiology 2018 39(10):1848-1853.

[2] F. J. A. Mont`Alverne, F. O. Lima, F. de Araújo Rocha, D. de Almeida Bandeira, A. F. de Lucena, H. C. Silva, J. S. Lee, R. G. Nogueira. Unfavorable vascular anatomy during endovascular treatment of stroke: challenges and bailout strategies. Journal of Stroke 2020;22(2):185-202.

[3] B. Gleich, I. Schmale, T. Nielsen, and J. Rahmer. Miniature magneto-mechanical resonators for wireless tracking and sensing. Science 2023;380:966-971.

[4] F. Fischer, C. Gletter, M. Jeong, and T. Qiu. Magneto-oscillatory localization for small-scale robots. npj Robot 2024;2.

[5] N. Hackelberg, J. Schumacher, M. Graeser, and T. Knopp. A Flexible High-Performance Signal Generation and Digitization Plattform based on Low-Cost Hardware. International Journal on Magnetic Particle Imaging 2022;8(1 Suppl 1).

[6] B. F. Edwards, D. M. Riffe, J. Y. Ji, and W. A. Booth. Interactions between uniformly magnetized spheres. American Journal of Physics 2017;85(2), 130-134.